Available online at www.sciencedirect.com
ScienceDirect
Diabetes & Metabolism 33 (2007) 296–302
Diabetes & Metabolism
http://france.elsevier.com/direct/diabet

Original article

Sources of endogenous glucose production in the Goto–Kakizaki diabetic rat

C.M. Sena[a,*], C. Barosa[b], E. Nunes[a], R. Seiça[a], J.G. Jones[b]

[a] *Institute of Physiology, Faculty of Medicine, University of Coimbra, Rua Larga, 3004-504 Coimbra, Portugal*
[b] *Center for Neuroscience and Cell Biology and Department of Biochemistry, Faculty of Sciences and Technology, Box 3126, University of Coimbra, 3001-401 Coimbra, Portugal*

Received 5 December 2006; accepted 18 March 2007
Available online 05 June 2007

Abstract

Plasma glucose, insulin and glucose tolerance were quantified in diabetic Goto–Kakizaki (GK) rats (342 ± 45 g, n = 5) and compared with weight-matched non-diabetic Wistars (307 ± 30 g, n = 8). Compared to Wistars, GK rats had higher fasting plasma insulin (219 ± 50 versus 44 ± 14 pmol/l, $P < 0.002$) and glucose (9.2 ± 2.3 versus 5.5 ± 0.5 mmol/l, $P < 0.025$). GK rats showed impaired glucose tolerance (IPGTT 2 h plasma glucose = 14 ± 1.5 versus 6.4 ± 0.1 mmol/l, $P < 0.001$). Endogenous glucose production (EGP) from glycogenolysis, phosphoenolpyruvate (PEP) and glycerol after 6 hours of fasting was quantified by a primed infusion of [U–^{13}C]glucose and $^{2}H_2O$ tracers and $^{2}H/^{13}C$ NMR analysis of plasma glucose. EGP was higher in GK compared to Wistar rats (191 ± 16 versus 104 ± 27 μmol/kg per min, $P < 0.005$). This was sustained by increased gluconeogenesis from PEP (85 ± 12 versus 35 ± 4 μmol/kg per min, $P < 0.02$). Gluconeogenesis from glycerol was not different (20 ± 3 in Wistar versus 30 ± 6 μmol/kg per min for GK), and glycogenolysis fluxes were also not significantly different (76 ± 23 μmol/kg per min for GK versus 52 ± 19 μmol/kg per min for Wistar). The Cori cycle accounted for most of PEP gluconeogenesis in both Wistar and GK rats (85 ± 15% and 77 ± 10%, respectively). Therefore, increased gluconeogenesis in GK rats is largely sustained by increased Cori cycling while the maintenance of glycogenolysis indicates a failure in hepatic autoregulation of EGP.

Résumé

Sources de production endogène du glucose chez le rat diabétique Goto–Kakizaki

La glycémie, l'insulinémie et la tolérance au glucose ont été mesurées chez des rats diabétiques Goto–Kakizaki (GK; 342 ± 45 gr, n = 5), comparés à des rats non diabétiques Wistar (307 ± 30 gr, n = 8). Comparés aux rats Wistar, les rats GK avaient des valeurs plus élevées à jeun de la glycémie et de l'insulinémie (respectivement 219 ± 50 versus 44 ± 14 pmol/l, $P < 0{,}002$, et 9,2 ± 2,3 *vs* 5,5 ± 0,5 mmol/l, $P < 0{,}025$). Les rats GK présentaient une diminution de la tolérance au glucose (IPGTT 2 hr glucose plasmatique : 14 ± 1,5 versus 6,4 ± 0.1 mmol/l, $P < 0{,}001$). La production endogène de glucose (PEG) à partir de la glycogénolyse, de la phosphoénolpyruvate (PEP) et du glycérol, après 6 heures de jeûne, a été mesurée après une perfusion de [U–^{13}C]glucose et du traceur $^{2}H_2O$, et analyse par RMN de glucose $^{2}H/^{13}C$ plasmatique. La PEG était plus élevée chez les rats GK comparés aux rats Wistar (191 ± 16 versus 104 ± 27 μmol/kg per min, $P < 0{,}005$), du fait d'une augmentation de la néoglucogenèse à partir du PEG (85 ± 12 versus 35 ± 4 μmol/kg per min, $P < 0{,}02$). La néoglucogenèse à partir du glycérol n'était pas différente (20 ± 3 chez les rats Wistar *vs* 30 ± 6 μmol/kg per min chez les rats GK), alors que le flux de la glycogénolyse avait tendance à être plus élevé chez les rats GK (76 ± 23 μmol/kg per min), comparés aux rats Wistar (52 ± 19 μmol/kg per min, $P = 0{,}06$). Le cycle de Cori était responsable de la plus grande partie de la néoglucogenèse à partir de la PEP chez les deux types de rats, Wistar et GK (respectivement 85 ± 15 % et 77 ± 10 %).

Ainsi, l'augmentation de la néoglucogenèse observée chez les rats GK est liée largement à l'augmentation du cycle de Cori, alors que le maintien de la glycogénolyse indique un déficit de l'autorégulation hépatique de la production endogène de glucose.

* Corresponding author.
E-mail address: csena@ci.uc.pt (C.M. Sena).

1262-3636/$ - see front matter © 2007 Elsevier Masson SAS. All rights reserved.
doi:10.1016/j.diabet.2007.03.002

Keywords: Endogenous glucose production; Gluconeogenesis; [U–^{13}C]glucose; Type 2 diabetes; Goto–Kakizaki rats; Wistar rats

Mots clés : Production endogène de glucose ; Néoglucogenèse ; Eau deutérée ; Diabète de type 2 ; Rat Goto–Kakizaki ; Rat Wistar

1. Introduction

Non-insulin-dependent, or Type 2 diabetes (T2D), is a disease characterized by multiple defects in systemic glucose metabolism. Fasting hyperglycaemia is a hallmark feature that significantly contributes to both morbidity and mortality of T2D patients. For this reason, control of plasma glucose levels is a key target for both nutritional and pharmacological interventions. To gain better insights into the underlying mechanisms and to test possible interventions of hyperglycaemia, the development of suitable animal models is crucial. Rodent strains that inherently develop T2D, such as the Zucker Diabetic Fatty and Goto–Kakizaki (GK) rats are valuable experimental models. The GK strain shares some important characteristics of human T2D with respect to systemic glucose metabolism. GK rats develop fasting hyperglycaemia, an impaired secretion of insulin in response to glucose, and insulin resistance of hepatic and peripheral tissues [1–4]. Less characterized in the GK model is the role of endogenous glucose production (EGP) and gluconeogenic fluxes in the development of fasting hyperglycaemia. In humans, elevated rates of EGP have been measured in overnight-fasted T2D patients with severe fasting hyperglycaemia. These abnormally high GP fluxes are largely fuelled by increased rates of glucose synthesis from gluconeogenesis [5,6]. Endogenous sources of gluconeogenesis include lactate derived via the Cori cycle, glycerol derived from hydrolysis of triglycerides, and gluconeogenic amino acids derived from proteolysis. Lactate and gluconeogenic amino acids are converted to glucose via the anaplerotic pathways of the Krebs cycle, while glycerol enters upstream at the level of triose phosphates. Elevated rates of Cori cycle fluxes have been reported in T2D [7]. The availability of glycerol may be increased in T2D as a result of increased triglyceride hydrolysis. However, it is not currently known if glycerol gluconeogenesis is elevated in T2D.

The contribution of glycogen, glycerol gluconeogenesis and phosphoenolpyruvate (PEP)-derived gluconeogenesis to fasting EGP can be quantified from analysis of ^{2}H-enrichment in positions 2, 5 and 6 of glucose following ingestion of $^{2}H_2O$ [8]. This method is considered to be an improvement on earlier measurements based on carbon tracers because 1): the ^{2}H enrichment distribution of glucose reflects the contribution of all gluconeogenic precursors, and 2): the ubiquitous distribution of $^{2}H_2O$ means that all gluconeogenic activity in the body is assayed. By combining $^{2}H_2O$ with a second tracer of glucose turnover such as [U–^{13}C]glucose, fractional gluconeogenic and glycogenolytic fluxes can be converted to absolute values [9]. In addition, Cori cycle contributions to gluconeogenesis can be quantified by analysis of recycled [U–^{13}C]glucose isotopomers [9–11]. In this report, we quantified fasting EGP from gluconeogenic and non-gluconeogenic sources and resolved the Cori cycle contribution to gluconeogenic PEP synthesis in GK diabetic rats. Our measurements revealed significant differences in glucose kinetics and sources between diabetic GK and Wistar control rats.

2. Methods

2.1. Animal studies

Five male GK rats and eight male Wistar control animals between 12 and 14 weeks of age were studied. The GK rats were obtained from a local breeding colony. All rats were fed ad libitum with a standard commercial pellet chow diet (diet AO4-Panlab) and allowed free access to water. During this time, they were subjected to a constant daily cycle of 12 hours light and 12 hours of dark. Fasting was initiated at the start of the light cycle by removal of food. Intraperitoneal glucose tolerance tests (1.75 g/kg of glucose, in the form of a 30% aqueous solution, was given by intraperitoneal injection), fasting plasma glucose, and insulin determinations were performed in all animals. For these measurements, a blood sample was taken during the first 6 hours of fasting for a baseline measurement of blood glucose and insulin levels. Blood glucose levels were determined with a glucometer (Elite-Bayer, Portugal). Plasma insulin levels were quantified by an in-house ELISA assay. To assess insulin resistance in the fasted state, the homeostasis model assessment of insulin resistance (HOMA-IR), was calculated, since this measurement has been shown to be well correlated with hyperinsulinemic–euglycemic clamp measurements of insulin sensitivity [12,13]. HOMA-IR was calculated as $[(I_f) \times (G_f)]/22.5$, where (I_f) is the fasting insulin level and (G_f) is the fasting glucose level [13]. This method has been validated only in humans, although several authors have used it in rats [36,37] and it is know from the literature that adult GK rat are insulin-resistant [4,38,39].

For analysis of EGP, rats were given a 3 ml injection of 99% $^{2}H_2O$ in 0.9% saline solution at 4.5 hours of fasting and a primed infusion of [U–^{13}C]glucose (62 μmol/kg, prime, 2.3 μmol/kg per min constant infusion for 90 min). For the constant infusion, [U–^{13}C]glucose was dissolved at a concentration of 16 μmol/ml in 0.9% saline containing 99% $^{2}H_2O$ and was infused at 0.04 ml/min. At 6 hours, rats were terminally anesthetized and blood was recovered via cardiac puncture. Blood was stored at 4 °C and centrifuged within 1 hour of being drawn.

2.2. Plasma glucose processing

The plasma supernatant protein was precipitated by centrifugation following addition of 1/10th the plasma volume of 70% perchloric acid. The supernatant was neutralized with

KOH and lyophilized following removal of $KClO_4$ by centrifugation. For conversion of plasma glucose to the monoacetone derivative, the lyophilized extracts were treated with 3 ml anhydrous acetone enriched to which concentrated sulfuric acid (4% v/v) was added in the cold. The mixture was stirred for 4 hours at room temperature, and was then quenched with 5 ml water. The diacetone glucose formed was hydrolyzed to monoacetone glucose by adjusting the pH to 2.1 with sodium carbonate and stirring for 5 hours at 40 °C. The pH was adjusted to 8.0 with sodium carbonate, the solvent was removed by rotary evaporation and monoacetone glucose was extracted from the dried residue with a few milliliters of boiling ethyl acetate or 1–2 ml of 95% acetonitrile/5% H_2O. After evaporation, the residue was dissolved in 0.6 ml of 95% acetonitrile–5% water containing a few grains of sodium bicarbonate and placed in a 5 mm NMR tube.

2.3. NMR spectroscopy

NMR spectra were acquired at 11.75 T with a Varian Unity 500 system equipped with a 5-mm broadband "switchable" probe with z-gradient (Varian, Palo Alto, CA). ^2H was observed with the 'broadband' coil tuned to the ^2H carrier frequency. Shimming was performed on the ^1H signal using manual adjustment in response to the ^1H-linewidths of selected resonances. Proton-decoupled ^2H NMR spectra were obtained without lock at 50 °C with a 1.6 s acquisition time. Under these conditions, the monoacetone glucose ^2H nuclei have T_1 values of ~ 0.2 s and are therefore fully relaxed before pulsing. The number of free-induction decays acquired for MAG derived from blood samples ranged from 20,000 to 40,000 (6.7–13.4 hours). Following ^2H NMR spectroscopy, ~25% of the acetonitrile solvent in the NMR sample was evaporated and replaced with deuterated acetonitrile. Partially relaxed, proton-decoupled ^{13}C NMR spectra were then obtained with a field-frequency lock. Spectra were acquired with a 60° pulse angle, an acquisition time of 2.5 s, a spectral width of 25 kHz (200 ppm), and a pulse delay of 0.5 s. Number of scans ranged from 4,000 to 16,000 (3.3–13.3 hours). The relative areas of selected peaks in both ^{13}C and ^2H NMR spectra were analyzed using the curve-fitting routine supplied with the NUTS PC-based NMR spectral analysis program (Acorn NMR Inc., Fremont, CA).

2.4. Quantifying EGP and Cori cycle flux from [U–^{13}C]glucose

Enrichment of plasma glucose from infused [U–^{13}C]glucose ($\mathbf{E_p}$) was determined from the carbon 1 multiplet of the ^{13}C NMR signal of MAG [9]. EGP was calculated as follows:

$$\text{EGP} = [\text{i} \times (\mathbf{E_i}/\mathbf{E_p})] - \text{i}$$

where i = infusion rate of [U–^{13}C]glucose in μmol/kg per min and $\mathbf{E_i}$ is the percent enrichment of infusate [U–^{13}C]glucose. EGP is reported as μmol/kg per min.

Cori cycle flux was estimated from the enrichment levels of plasma glucose triose ^{13}C-isotopomers (E_{triose}) relative to the plasma [U–^{13}C]glucose precursor pool (E_p) multiplied by EGP. A correction factor of 1.5 was used to account for dilution at the level of the oxaloacetate pool of the hepatic Krebs cycle [14].

$$\text{Cori cycle flux}(\mu\text{mol/kg per min}) = \text{EGP} \times 1.5 \times (E_{triose}/E_p)$$

2.5. Gluconeogenic and glycogenolytic fluxes

The fractional contribution of glycogenolysis, glycerol gluconeogenesis and gluconeogenesis from all other sources to EGP was estimated directly from the ratio of deuterium signal intensities of hydrogens 2, 5 and 6S (H2, H5 and H6S) of the ^2H NMR spectrum of MAG [15–17].

$$\text{Fraction of EGP from glycogenolysis}(F_{glycogen}) = 1 - (\text{H5}/\text{H2})$$
$$\text{Fraction of EGP from glycerol}(F_{glycerol}) = (\text{H5} - \text{H6S})/\text{H2}$$
$$\text{Fraction of EGP from PEP}(F_{PEP}) = (\text{H6S}/\text{H2})$$

Absolute gluconeogenic and glycogenolytic fluxes were calculated by multiplying the fractional rates by EGP. Units are μmol/kg per min of hexose equivalents.

$$\text{Glycogenolysis flux} = \text{EGP} \times (F_{glycogen})$$
$$\text{Glycerol gluconeogenesis flux} = \text{EGP} \times (F_{glycerol})$$
$$\text{PEP gluconeogenesis flux} = \text{EGP} \times (F_{PEP})$$

3. Results and discussion

3.1. Physiological characteristics

GK rats consistently developed the hallmark features of T2D as they aged. At 12 weeks of age, GK rats had reduced body weight and elevated fasting plasma glucose levels. Usually our animal model of T2D has slightly lower body weight when compared to age-matched Wistar rats (data not shown). They also had reduced insulin sensitivity (or increased insulin resistance) as reflected by significantly higher values of HOMA-IR compared with the Wistar controls. Plasma glucose levels following a glucose load were consistently higher in the GK diabetic rats indicating impaired glucose tolerance (IPGTT) (see Table 1). This is consistent with other reports in the literature in this animal model of T2D [4,38–40]. The GK rats show statistically significant increases in total and HDL-cholesterol, no changes in triglycerides and they were not ketotic (data not shown).

3.2. Rates and Sources of EGP

Following [U–^{13}C]glucose infusion, mean plasma glucose enrichment levels of [U–^{13}C]glucose were 2.2 ± 0.7% for Wistar

Table 1
Metabolic parameters and sources of EGP parameters for Wistar control and diabetic GK rats. Data are presented as mean ± S.D.

Parameters	Wistar (n = 8)	GK rats (n = 5)	P values
Body weight (g)	307 ± 14	342 ± 20	0.1800
Fasting blood glucose (mmol/l)	5.5 ± 0.1	9.1 ± 1.0**	0.0220
Blood glucose 2 hours after IPGTT (mmol/l)	6.4 ± 0.08	13.8 ± 1.5***	0.000002
Fasting blood insulin (pmol/l)	44 ± 6	219 ± 22***	0.0010
HOMA-IR (μU/ml × mmol/l)	1.56 ± 0.38	12.46 ± 1.11***	0.0005
EGP (μmol/kg per min)	104 ± 11	191 ± 16***	0.0021
Glucose production from PEP (μmol/kg per min)	35 ± 4	85 ± 12**	0.0113
Glucose production from glycerol (μmol/kg per min)	20 ± 3	30 ± 6	0.1825
Glucose production from glycogen (μmol/kg per min)	50 ± 8	76 ± 10	0.0594
Cori cycle flux (μmol/kg per min)	31 ± 7	63 ± 10*	0.0264

*$P < 0.05$ compared to controls; **$P < 0.025$ compared to controls; ***$P \leq 0.001$ compared to controls.

and 1.2 ± 0.1% for GK rats. Given the similar body weights between the two groups, the lower [U–^{13}C]glucose enrichment in the GK rats reflects an increased dilution of the tracer due to higher EGP rates. For the 6-hour fasted control animals, EGP rates of ~100 μmol/kg per min were obtained. In comparison, values of 114–120 μmol/kg per min were obtained from 5-hour fasted anesthetized rats using [3-^{3}H]glucose [18]. Given that the animals used in this study weighed 220–240 g, and were therefore substantially smaller than the 307 g of our study animals, the higher EGP values of Mithieux et al. compared to our estimates may be at least partially due to the inherently higher basal metabolic rates of the smaller rats [19]. In a study of 6-hour fasted, conscious rats of similar weights to that used in our study (~300 g), EGP rates of 70–80 μmol/kg per min were reported [20]. Given that anesthesia is accompanied by a decrease in insulin secretion [21], the higher EGP values observed in our study compared to that or Neese et al. may be attributable to incomplete suppression of EGP as a result of reduced insulin levels. Moreover, the anesthetic cocktail used did not produce hyperglycaemia per se in Wistar rats since these animals exhibited low glucose levels but may have reduced the clearance of high glucose levels in the blood of GK rats. A similar type of dissociative anesthesia (ketamine + xylazine mixture) was recently shown to induce hyperglycaemia in fed, but not fasted, Sprague–Dawley rats [41], suggesting this type of anesthesia may affect the clearance of circulating blood glucose but not stimulate its production.

EGP values for 6-hour fasted diabetic GK rats were almost double that of control animals (Table 1), averaging 190 μmol/kg per min. Previous studies using both basal and clamp conditions have shown that hepatic glucose production is increased in this animal in vivo (Refs. [4] and [39]), although the responsible mechanism has not yet been totally clarified. In a study of conscious ZDF rats infused with [6-^{3}H]glucose, post-absorptive EGP rates of 134 and 101 μmol/kg per min were reported at 3 and 10 hours of fasting, respectively [22]. No data were presented for control animals under the same conditions. In 24-hour fasted anesthetized ZDF rats weighing ~450 g, EGP rates of ~90 μmol/kg per min were reported, approximately double the rate measured from control animals of matching age [23].

In summary, EGP can be substantially influenced by fasting state, animal weight and anesthesia. To the extent that these factors were consistent for non-diabetic control and T2D rat models, the differences in EGP that were observed between healthy and GK rats can be attributed to the pathophysiology of the GK diabetic animal.

During the post-absorptive state, EGP is derived from a combination of glycogenolysis and gluconeogenesis. Analysis of plasma glucose ^{2}H-enrichment distributions from the $^{2}H_2O$ tracer allows the contributions of glycogen, glycerol gluconeogenesis and gluconeogenesis derived via PEP to be determined [8]. For control rats, total gluconeogenesis contributed about 50% of EGP at 6 hours of fasting. This is in good agreement with a mass-isotopomer distribution analysis study which reported a gluconeogenic contribution of 51% to EGP at 5–6 hours of fasting [20] but less than the 71% reported by Burgess et al. [24] using the same $^{2}H_2O$ methodology as ours. These different estimates of fractional gluconeogenesis may be at least partially due to differences in body weights of the animals (225 g for the study of Burgess et al. versus 307 g for our study and 300 g for the study of Neese et al.). Hepatic glycogen may be more rapidly depleted in the smaller animals as a result of higher basal metabolic rates. As a result, the fractional contribution of glycogenolysis to EGP would be reduced while that of gluconeogenesis would be correspondingly increased for the smaller versus the larger animals. From the $^{2}H_2O$ enrichment distribution of glucose hydrogen 5 and 6, the gluconeogenic fraction can be resolved into contributions from glycerol and PEP [8]. For control animals, hydrogen 6 relative enrichments approached those of hydrogen 5 (Table 2) indicating that most of the gluconeogenic carbons originated via PEP and the Krebs cycle with only minor contributions from glycerol [8]. The relative contributions of glycerol gluconeogenesis, PEP-gluconeogenesis and glyco-

Table 2
^{2}H relative enrichments of hydrogens 1–6 of plasma glucose from Wistar control (n = 8) and GK diabetic rats (n = 5) derived from the relative areas of the ^{2}H NMR signals of MAG. Enrichment of position 2 is arbitrarily set to 100 and the uncertainties (±) represent standard deviations

	Relative ^{2}H enrichment of glucose hydrogens						
	1	2	3	4	5	6R	6S
Wistar control	47 ± 4[d]	100	40 ± 6[b]	52 ± 3	53 ± 4	35 ± 4	34 ± 4
GK diabetic	44 ± 3	100	41 ± 4[c]	50 ± 5	60 ± 5[a]	37 ± 5	44 ± 4

[a] Significantly different from the corresponding relative enrichment of Wistar controls ($P < 0.05$).
[b] Significantly different from hydrogen 5 relative enrichment ($P < 0.005$).
[c] Significantly different from hydrogen 5 relative enrichment ($P < 0.02$).
[d] Significantly different from either hydrogen 6S or hydrogen 6R relative enrichments ($P < 0.025$).

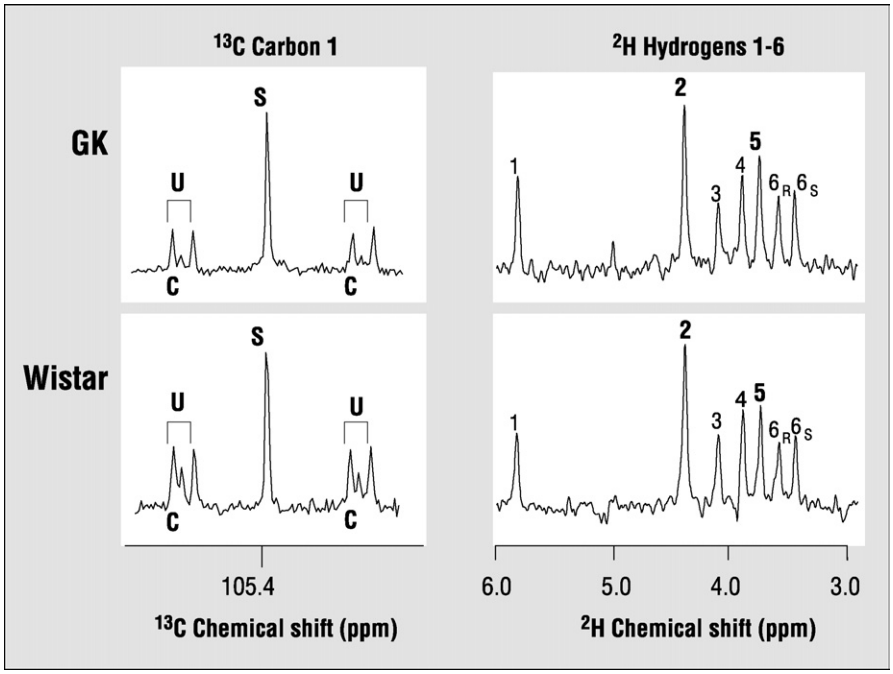

Fig. 1. ^{13}C and ^{2}H NMR signals of MAG prepared from plasma glucose of a Wistar control and a GK diabetic rat. In each case, the ^{13}C signal from carbon 1 of MAG is shown on the left hand side and the ^{2}H signals of hydrogens 1–6 are shown on the right-hand side. For the ^{13}C signal, the natural abundance singlet contribution (S), the multiplet component originating from [U–^{13}C]glucose (U) and the multiplet components arising from partially-labeled glucose molecules generated via Cori cycle (C) are indicated. For the ^{2}H spectra, the number above each signal represents the position of the deuterium nuclei in the original glucose skeleton.

genolysis to EGP resembles that obtained from overnight-fasted healthy humans using the $^{2}H_2O$ measurement [8,15,16,25]. From the relative intensity of the doublet signal assigned to recycled ^{13}C-triose units derived via the Cori cycle (see Fig. 1) , the excess enrichment from recycled triose units (E_{triose}) was estimated to be 0.37 ± 0.10%. The contribution of the Cori cycle to EGP as determined from the ratio of E_{triose} to [U–^{13}C]glucose enrichments was comparable to that of PEP gluconeogenesis derived from the ^{2}H NMR analysis. This indicates that gluconeogenic PEP carbons were mostly derived from Cori cycle activity.

In the GK diabetic rats, gluconeogenesis from PEP was more than twice that of the control group. Cori cycle fluxes were also increased, but these estimates have higher uncertainties compared to those of control animals. As illustrated by Fig. 1, the doublet signal representing E_{triose} was lower in GK rats compared to controls as a result of the increased dilution from EGP. The signal-to-noise ratio of the E_{triose} doublet was ~5:1, hence on this basis, the precision of our measurement is at best ± 20% of the real signal intensity. Consequently, this imposes a minimum uncertainty of ± 20% on estimates of Cori cycle fluxes. Glycerol gluconeogenesis rates and glycogenolytic fluxes were not significantly different between GK and control groups.

3.3. *^{2}H enrichment patterns of plasma glucose from $^{2}H_2O$*

The relative ^{2}H-enrichments of plasma glucose from Wistar control and GK diabetic rats are shown in Table 2. Hydrogen 2 had the largest signal intensity, reflecting extensive equilibration of glucose hydrogen 2 and body water. Enrichment of the other glucose hydrogens ranged from ~35% to 70% of hydrogen 2, reflecting differences in the gluconeogenic contribution to GP as well as differences in the extent of exchange between the hydrogens of body water and those of gluconeogenic intermediates. Next to hydrogen 2, hydrogen 5 was the most highly enriched, reflecting the stoichiometric incorporation of water hydrogen at the level of enolase and/or triose phosphate isomerase during gluconeogenesis from PEP and glycerol [8]. Enrichment of hydrogen 3 was significantly less than hydrogen 5, which may reflect exchange of fructose-6-P and triose P via transaldolase [26]. Similar differences between hydrogen 5 and hydrogen 3 enrichment levels of plasma glucose from $^{2}H_2O$ have been observed in fasted humans [15,16]. The reduced enrichment in hydrogen 3 relative to hydrogen 5 was observed in both Wistar control and diabetic GK rats. The glucose hydrogen 3:2 ^{2}H-enrichment ratios (H3/H2) of the Wistar controls were in good agreement with plasma glucose measurements from a previous $^{2}H_2O$ labeling study of 6-h fasted healthy Sprague–Dawley rats, where H3/H2 was quantified by ^{2}H NMR analysis of the gluconate derivative of plasma glucose [27]. Hydrogen 4 enrichments were equivalent to those of hydrogen 5, consistent with extensive equilibration of the NADH reducing hydrogen with that of body water and/or aldolase-catalyzed exchange of glyceraldehyde-3-phosphate hydrogen 1 with that of body water [28]. In control rats, hydrogen 1 enrichments were significantly higher than either of the prochiral hydrogen 6 sites, while GK animals had no differences in hydrogen 1 and 6 enrichment levels. In healthy humans, hydrogen 1 enrichments were also found to be significantly higher than the average of the hydrogen 6 enrichments [15,16,29]. Lastly, the prochiral hydrogen 6 sites of glucose

were enriched to equal levels, resembling the distributions observed in both healthy and cirrhotic humans [15,16].

In the diabetic GK rat, post-absorptive EGP rates are nearly doubled over control values. A similar magnitude difference in EGP rate was reported between ZDF and control rats after 24-hours of fasting. In comparison, overnight-fasted T2D patients have EGP rates that are typically 20–30% higher than those of healthy controls [5,6,30]. Therefore, while both GK and ZDF rat models of T2D exhibit increased fasting EGP, the relative increase compared to control values is much bigger compared to the human counterparts. Among other things, this may be an important consideration if modification of EGP in these rat models by hormonal or pharmacological intervention is extrapolated to humans.

In the GK rat, the principal mechanism of increased EGP during post-absorptive conditions is an increase in glucose recycling via the Cori cycle. Increased Cori cycle activity has also been reported for T2D patients [31,32] and would therefore also contribute to increased gluconeogenic flux through PEP. Whether an increase in Cori cycle activity entirely accounts for the increased gluconeogenic flux in T2D patients is not known. In non-diabetic but insulin-resistant obese subjects, increased gluconeogenic flux via PEP was associated with elevated protein catabolic rates [33]. This suggests the possibility that gluconeogenic amino acids derived from protein catabolism could also contribute to increased PEP flux in T2D patients.

In the GK rats, hepatic glycogenolytic rates were maintained in the face of increased gluconeogenic fluxes. This indicates that the reciprocal inhibition of glycogenolysis in response to an increase in gluconeogenesis, also referred to as the hepatic autoregulation of glucose output, is defective. A similar defect in the hepatic autoregulation of glycogenolysis has also been observed in both obese and non-obese T2D patients with severe hyperglycaemia (defined as plasma glucose ≥ 9 mM) studied under baseline conditions [5,34,35]. Basu et al. [35] demonstrated that a reduced sensitivity of glycogen phosphorylase to inhibition by insulin is a contributing mechanism to this defect. In T2D patients with less severe hyperglycaemia, hepatic autoregulation is better preserved [5].

Elevated fasting EGP is a common feature of both GK and ZDF rat models of T2D. However, the portfolio of endogenous glucose sources appears to be quite different for each model. Our results indicate that for diabetic GK rats, the increase in post-absorptive EGP is largely fuelled by an increase in Cori cycling of glucose. In marked contrast, the increase in EGP over control rates for 24-hours ZDF rats is entirely sustained by an elevation of hepatic glycogenolysis, with no significant changes in gluconeogenic fluxes from either PEP or glycerol [23]. These flux measurements have not been reported for 6-hour fasted animals, but on the basis of higher hepatic glycogen levels (276 μmol/g wet weight liver for non-fasted ZDF rats [22] compared to 113 μmol/g wet weight liver for 24-hour fasted animals [23] EGP from glycogenolysis is expected to be even higher during the post-absorptive period compared to 24-hours of fasting.

4. Conclusions

We demonstrated that sources of endogenous glucose synthesis from glycogen, glycerol, PEP and the Cori cycle could be quantified in a rat model of T2D by a combination of [U–^{13}C]glucose and $^{2}H_2O$ tracers coupled with ^{2}H and ^{13}C NMR analysis of plasma glucose. In healthy 6-hour fasted rats, the contribution of gluconeogenic fluxes and glycogenolysis to fasting glucose production resembled that obtained from overnight-fasted humans while in the GK rat, there is an increased role of gluconeogenesis and the Cori cycle in EGP. These findings are highly consistent with $^{2}H_2O$ studies of severely hyperglycemic T2D patients and provide additional validation for the GK rat as a model for investigating hepatic glucose metabolism in T2D.

Acknowledgments

This work was supported by a Marie Curie Fellowship of the European Community program: Improving Human Research Potential and the Socioeconomic Knowledge Base under contract number HPMFCT-2000-00469, the Juvenile Diabetes Research Foundation International (JDRF1-5-2004-306) and the Portuguese Foundation of Science and Technology (POCTI-QUI-55603-2004). We wish to thank Professor João Patrício and co-workers (Laboratory of Animals Research Center, University Hospitals, Coimbra) for maintaining the animals and also Maria de Lurdes Silva for her technical assistance.

References

[1] Goto Y-I, Sasaki M, Ono T, Abe S. GK rat as a model of nonobese, noninsulin dependent diabetes: selective breeding over 35 generations. In: Frontiers in diabetes research. Lessons from animal diabetes II. London: John Libbey; 1988.

[2] Goto Y, Kakizaki M, Masaki N. Spontaneous diabetes produced by selective breeding of normal Wistar rats. Proc Jpn Acad 1975;51:80–5.

[3] Kimura K, Toyota T, Kakizaki M, Kudo M, Takebe K, Goto Y. Impaired insulin secretion in the spontaneous diabetes rats. Tohoku J Exp Med 1982;137:453–9.

[4] Picarel-Blanchot F, Berthelier C, Bailbe D, Portha B. Impaired insulin secretion and excessive hepatic glucose production are both early events in the diabetic GK rat. Am J Physiol 1996;271:E755–62.

[5] Boden G, Chen X, Stein TP. Gluconeogenesis in moderately and severely hyperglycemic patients with type 2 diabetes mellitus. Am J Physiol 2001;280:E23–30.

[6] Gastaldelli A, Baldi S, Pettiti M, Toschi E, Camastra S, Natali A, et al. Influence of obesity and type 2 diabetes on gluconeogenesis and glucose output in humans. a quantitative study. Diabetes 2000;49:1367–73.

[7] Tayek JA, Katz J. Glucose production, recycling, and gluconeogenesis in normals and diabetics. a mass isotopomer [U–^{13}C]glucose study. Am J Physiol 1996;270:E709–17.

[8] Landau BR, Wahren J, Chandramouli V, Schumann WC, Ekberg K, Kalhan SC. Contributions of gluconeogenesis to glucose production in the fasted state. J Clin Invest 1996;98:378–85.

[9] Perdigoto R, Rodrigues TB, Furtado AL, Porto A, Geraldes C, Jones JG. Integration of [U–^{13}C]glucose and $^{2}H_2O$ for quantification of hepatic glucose production and gluconeogenesis. NMR Biomed 2003;16:189–98.

[10] Katz J, Tayek JA. Recycling of glucose and determination of the Cori cycle and gluconeogenesis. Am J Physiol 1999;277:E401–7.

[11] Haymond MW, Sunehag AL. The reciprocal pool model for the measurement of gluconeogenesis by use of [U–^{13}C]glucose. Am J Physiol 2000; 278:E140–5.

[12] Katz A, Nambi SS, Mather K, Baron AD, Follmann DA, Sullivan G, et al. Quantitative insulin sensitivity check index: a simple, accurate method for assessing insulin sensitivity in humans. J Clin Endocrin & Metab 2000;85:2402–10.

[13] Matthews DR, Hosker JP, Rudenski AS, Naylor BA, Treacher DF, Turner RC. Homeostasis model assessment—insulin resistance and beta-cell function from fasting plasma glucose and insulin concentrations in man. Diabetologia 1985;28:412–9.

[14] Mendes AC, Caldeira MM, Silva C, Burgess SC, Merritt ME, Gomes F, et al. Hepatic UDP-glucose ^{13}C isotopomers from [U–^{13}C]glucose. A simple analysis by ^{13}C NMR of urinary menthol glucuronide. Magn Res Med 2006;56:1121–5.

[15] Perdigoto R, Furtado AL, Porto A, Rodrigues TB, Geraldes C, Jones JG. Sources of glucose production in cirrhosis by $^{2}H_2O$ ingestion and ^{2}H NMR analysis of plasma glucose. Biochim Biophys Acta-Molecular Basis of Disease 2003;1637:156–63.

[16] Jones JG, Solomon MA, Cole SM, Sherry AD, Malloy CR. An integrated ^{2}H and ^{13}C NMR study of gluconeogenesis and TCA cycle flux in humans. Am J Physiol 2001;281:E848–51.

[17] Weis BC, Margolis D, Burgess SC, Merritt ME, Wise H, Sherry AD, et al. R. Glucose production pathways by ^{2}H and ^{13}C NMR in patients with HIV-associated lipoatrophy. Magn Res Med 2004;51:649–54.

[18] Mithieux G, Gautier-Stein A, Rajas F, Zitoun C. Contribution of intestine and kidney to glucose fluxes in different nutritional states in rat. Comp Biochem Physiol B Biochem Mol Biol 2006;143:195–200.

[19] Kleiber M, Smith AH, Chernikoff TN. Metabolic rate of female rats as a function of age and body size. Am J Physiol 1956;186:9–12.

[20] Neese RA, Schwarz JM, Faix D, Turner S, Letscher A, Vu D, et al. Gluconeogenesis and intrahepatic triose phosphate flux in response to fasting or substrate loads. Application of the mass isotopomer distribution analysis technique with testing of assumptions and potential problems. J Biol Chem 1995;270:14452–66.

[21] Vore SJ, Aycock ED, Veldhuis JD, Butler PC. Anesthesia rapidly suppresses insulin pulse mass but enhances the orderliness of insulin secretory process. Am J Physiol 2001;281:E93–9.

[22] van Poelje PD, Potter SC, Chandramouli VC, Landau BR, Dang Q, Erion MD. Inhibition of fructose 1,6-bisphosphatase reduces excessive endogenous glucose production and attenuates hyperglycaemia in Zucker diabetic fatty rats. Diabetes 2006;55:1747–54.

[23] Jin ES, Burgess SC, Merritt ME, Sherry AD, Malloy CR. Differing mechanisms of hepatic glucose overproduction in triiodothyronine-treated rats vs. Zucker diabetic fatty rats by NMR analysis of plasma glucose. Am J Physiol 2005;288:E654–62.

[24] Burgess SC, Nuss M, Chandramouli V, Hardin DS, Rice M, Landau BR, et al. Analysis of gluconeogenic pathways in vivo by distribution of ^{2}H in plasma glucose: comparison of nuclear magnetic resonance and mass spectrometry. Anal Biochem 2003;318:321–4.

[25] Burgess SC, Weis B, Jones JG, Smith E, Merritt ME, Margolis D, et al. Noninvasive evaluation of liver metabolism by ^{2}H and ^{13}C NMR isotopomer analysis of human urine. Anal Biochem 2003;312:228–34.

[26] Stingl H, Chandramouli V, Schumann WC, Brehm A, Nowotny P, Waldhausl W, et al. Changes in hepatic glycogen cycling during a glucose load in healthy humans. Diabetologia 2006;49:360–8.

[27] Jones JG, Carvalho RA, Sherry AD, Malloy CR. Quantitation of gluconeogenesis by ^{2}H nuclear magnetic resonance analysis of plasma glucose following ingestion of $^{2}H_2O$. Anal Biochem 2000;277:121–6.

[28] Rose I, O'Connell EL. Stereospecificity of the sugar-phosphate isomerase reactions—a uniformity. Biochim Biophys Acta 1960;42:159–60.

[29] Chandramouli V, Ekberg K, Schumann WC, Wahren J, Landau BR. Origins of the hydrogen bound to carbon 1 of glucose in fasting: significance in gluconeogenesis quantitation. Am J Physiol 1999;277:E717–23.

[30] Diraison F, Large V, Brunengraber H, Beylot M. Non-invasive tracing of liver intermediary metabolism in normal subjects and in moderately hyperglycaemic NIDDM subjects. Evidence against increased gluconeogenesis and hepatic fatty acid oxidation in NIDDM. Diabetologia 1998; 41:212–20.

[31] Tappy L, Acheson K, Curchod B, Schneiter P, Normand S, Pachiaudi C, et al. Overnight glucose-metabolism in obese non-insulin-dependent diabetic-patients and in healthy lean individuals. Clin Physiol 1994;14: 251–65.

[32] Tayek JA, Katz J. Glucose production, recycling, and gluconeogenesis in normals and diabetics: a mass isotopomer [U–^{13}C]glucose study. Am J Physiol 1996;270:E709–17.

[33] Chevalier S, Burgess SC, Malloy CR, Gougeon R, Marliss EB, Morais JA. The greater contribution of gluconeogenesis to glucose production in obesity is related to increased whole-body protein catabolism. Diabetes 2006;55:675–81.

[34] Gastaldelli A, Miyazaki Y, Pettiti M, Buzzigoli E, Mahankali S, Ferrannini E, et al. Separate contribution of diabetes, total fat mass, and fat topography to glucose production, gluconeogenesis, and glycogenolysis. J Clin Endocrinol Metab 2005;89:3914–21.

[35] Basu R, Chandramouli V, Dicke B, Landau B, Rizza R. Obesity and type 2 diabetes impair insulin-induced suppression of glycogenolysis as well as gluconeogenesis. Diabetes 2005;54:1942–8.

[36] Pickavance LC, Brand CL, Wassermann K, Wilding JP. The dual PPAR-alpha/gamma agonist, ragaglitazar, improves insulin sensitivity and metabolic profile equally with pioglitazone in diabetic and dietary obese ZDF rats. Br J Pharmacol 2005;144:308–16.

[37] Thulé PM, Campbell AG, Kleinhenz DJ, Olson DE, Boutwell JJ, Sutliff RL, et al. Hepatic insulin gene therapy prevents deterioration of vascular function and improves adipocytokine profile in STZ-diabetic rats. Am J Physiol 2006;290:E114–22.

[38] Berthelier C, Kergoat M, Portha B. Lack of deterioration of insulin action with aging in the GK rat: a contrasted adaptation as compared with non-diabetic rats. Metabolism 1997;46:890–6.

[39] Bisbis S, Bailbe D, Tormo MA, Picarel-Blanchot F, Derouet M, Simon J, et al. Insulin resistance in the GK rat: decreased receptor number but normal kinase activity in liver. Am J Physiol 1993;265:E807–13.

[40] Seiça RM, Suzuki KI, Santos RM, Rosário LM. Impaired insulin secretion in isolated islets of Goto–Kakizaki rats, an animal model of non obese type 2 diabetes, is a primary event. Acta Med Port 2004;17:42–8.

[41] Saha JK, Xia J, Engle SK, Chen YF, Glaesner W, Jakubowski JA. A model of controlled acute hyperglycaemia in rats: effects of insulin and glucagon-like peptide-1 analog. J Pharmacol Exp Ther 2006;316:1159–64.